Geometric limitations of 3D printed continuous flax-fiber reinforced biocomposites cellular lattice structures

Thomas Fruleux, Mickaël Castro, David Correa, Kui Wang, Ryosuke Matsuzaki, Antoine Le Duigou

Geometric limitations of 3D printed continuous flax-fiber reinforced biocomposites cellular lattice structures

Thomas Fruleux [a], Mickaël Castro [a], David Correa [b], Kui Wang [c], Ryosuke Matsuzaki [d], Antoine Le Duigou [a,*]

[a] *Institut de Recherche Dupuy de Lôme (IRDL UMR CNRS 6027), Bionics-group, Centre de Recherche Christian Huygens, Rue de Saint-Maudé, 56100 Lorient, France*
[b] *School of Architecture, University of Waterloo, 7 Melville Street S, N1S 2H4, Cambridge, Ontario, Canada*
[c] *School of Traffic and Transportation Engineering, Central South University (CSU), China*
[d] *Tokyo University of Science Noda Campus, 2641 Yamazaki 278-8510, Noda-shi, Chiba-ken, Japan*

ABSTRACT

3D-printing of biocomposites using continuous natural fiber composites is emerging as a relevant manufacturing method to develop highly tailorable materials. These are materials with high performance characteristics, whose capabilities have been achieved through the controlled design of the mesostructure via the 3D printing process. However, the development of 3D printing using continuous natural fiber composites is so recent that no geometric limitations have yet been investigated. The present article has established the printability and design window of several cellular lattice structures by investigating and discussing a comparative analysis of the difference between the programmed and actual trajectories of pure polylactic acid (PLA), short flax fiber biocomposite (FF/PLA) and continuous flax fiber/PLA biocomposites (cFF/PLA) for a specific set of printing and slicing parameters. It is expected that the presented findings will support the ongoing development of improved design methods and optimized technical deposition approaches that can expand the design space for cFF/PLA 3D printed biocomposites with multi-layered periodic cellular lattice patterns.

1. Introduction

3D-printing of biocomposites is a subset of 3D-printed composites that aims to limit the use of non-renewable resources in order to reduce its ecological footprint [1]. The production of continuous natural fiber reinforced filaments for 3D-printing has significantly improved the mechanical performance of composites compared to those reinforced with short fibers [2] and it has expanded the technical possibilities for shape-changing materials such as Hygromorph BioComposites (HBC) [3].

3D-printing represents a "material by design" approach in the manufacturing process with the highest degree of freedom as it enables the functional tailoring of the material's mesostructure, i.e the structure at the ply scale. This direct manipulation of the micro and meso-scale architecture of the material composition has been demonstrated to have a direct effect on the corresponding performance characteristics at multiple levels [4–6]. By designing the material organization through the deposition process, the structures are functionally graded to have the desired amount of material (thickness and width) and the intended

direction dependent properties that are optimal for the targeted application; following a similar model to that encountered in biological structures [7–11].

Although 3D-printing of cellular lattice structures are almost exclusively applied to metallic and polymeric materials, there has been an increasing amount of research into expanding the possibilities of short and continuous fibers composites [12–15]. Matsuzaki et al. [15] evidenced the difference between programmed and 3D-printed round-like structures for continuous carbon reinforced PolyAmide (cCF/PA) composites. By modifying the radius of the circles in the unit cell, they observed that the printed radius was always smaller than the programmed radius, which could be due to the twisting motion of the yarns during printing. Their numerical model evidenced that the stiffness of the filament due to the fiber content and the quadratic moment (diameter) were the key factors in producing high fidelity printed cCF/PA composites parts.

The present article emphasizes the geometric limitations of 3D printing continuous flax fiber/PLA biocomposites (cFF/PLA) when addressing patterns with small unit cells and tight curvature radius. This

Table 1

Extrusion parameters for the production of customized cFF/PLA filament.

Extrusion parameters	cFF/PLA filament
Die temperature (°C)	200
Oven temperature (°C)	120
Die size (mm)	0.6 (diameter) x 20 (length)
Puller speed (m/min)	1.00
Extrusion speed (rpm)	3

investigation presents valuable findings that can support improved methods to print high performance sustainable structures for technical applications using continuous fibres. Geometric limitations incorporate both limit printed angle and limit printed diameter of out-of-plane tubular and pentagonal architectures. By assessing the difference between programmed and real trajectories, it aims to identify general deviation characteristics, geometric limitations and best-practices that can improve material development, optimize printing variables and tool-path design methods for continuous fiber reinforced biocomposites with complex 3D-printed architectures. A comparison with pure polylactic acid (PLA) and short flax fiber polylactic acid (FF/PLA) 3D-printed parts will be presented. Finally, a discussion on future parameters to improve printing fidelity is initiated.

2. Materials and methods

Three types of filaments were used in this study: two commercial filaments in PLA (PLA Galaxy Silver filament supplied by Prusa®, diameter = 1.75 mm) and FF/PLA (PLA Flax filament supplied by Nanovia®, diameter = 1.75 mm) with a fiber volume fraction (FVF) of 7.0 ± 1.9 % while the last one was a customized cFF/PLA filament manufactured by co-extrusion. The cFF/PLA filament production was firstly developed by Le Duigou et al. [2]. For producing the customized filament, flax fiber bundle (supplied by Safilin®, linear density = 68 Tex) is conducted towards a heated nozzle by a drawing bench while PLA matrix is sheared and melted inside a single screw SCAMEX extruder before being introduced in the heat nozzle. Impregnation of flax bundle by PLA matrix is then performed. Extrusion parameters are described in Table 1. When leaving the nozzle, flax fiber bundle is surrounded by the matrix which solidifies as temperature decreases. The reliability of the filament production process is assessed through the continuous measurement of the filament diameter (around 500 μm) by ZUMBACH laser sensor. The final customized cFF/PLA filament is identical to the one used by Fruleux et al. [16] which contains a fiber

volume fraction of 32.6 ± 0.5 %.

The cellular lattice structures were first programmed on Full-Control_Gcode_Designer (open-source software for unconstrained design in additive manufacturing) and then printed using a PRUSA MK3s 3D-printer with a custom print head. Because of the difference in filament formulation, two nozzles were used, one for each type of filament: one commercial nozzle (d_n = 0.4 mm) for PLA and FF/PLA structures and one customized nozzle (d_n = 0.9 mm) for cFF/PLA structures. The printing and slicing parameters, nozzle temperature (T_n), bed temperature (T_b), layer height (LH) and layer number (LN) were kept consistent for both filaments at T_n = 190 °C, T_b = 60 °C, LH = 0.15 mm and LN = 50. Although adjusting some of these parameters such as printing temperature could have enhanced the printing fidelity, this was out of the scope of this study. The only printing parameters that were adjusted independently included the nozzle diameter (d_n) and printing speed in the straight paths and in the corners. Printing speeds were kept at 150 mm.min^{-1} in straight paths and 50 mm.min^{-1} in corners for cFF/PLA and 1000 mm.min^{-1} constantly for FF/PLA and PLA-structures respectively. These values were chosen for productivity purposes after verifying that no significant improvement was induced by decreasing the printing speed. Printing fidelity will be defined as the difference between the fixed (A_{th}) and printed (A_{exp}) areas by image analysis with the KEYENCE VHX-7000 digital microscope. Thickness variation between set and printed model was not investigated here since it has already been tackled in a former study [17]. Based on their results, it is clear that slicing parameters used in these experiments will ensure over-compaction of the filament resulting in a thicker thickness compared to preset values. Fig. 1 emphasizes structural parameters (thickness and diameter) useful to quantify both areas. Two closed shapes were selected to analyze printing fidelity: a circle and a polygon (regular and irregular octagon). While the circle was used to assess the minimum achievable diameter of a 3D-printed cylindrical structure (Fig. 2a), the polygons were used to identify the printable angle limit (Fig. 2b). These shapes were chosen both for technical reasons (easy Gcode programmability), existing bibliographical support and indicative structural features (diameter and angle) to quantify geometric limitations.

3. Results and discussion

The results shown in Fig. 2 illustrate the noticeable difference between the target tool path geometry and the resulting shape of the printed sample made with cFF/PLA, pure PLA and FF/PLA. The influence of the set diameter (Fig. 2a) to build tubular pieces is a particular

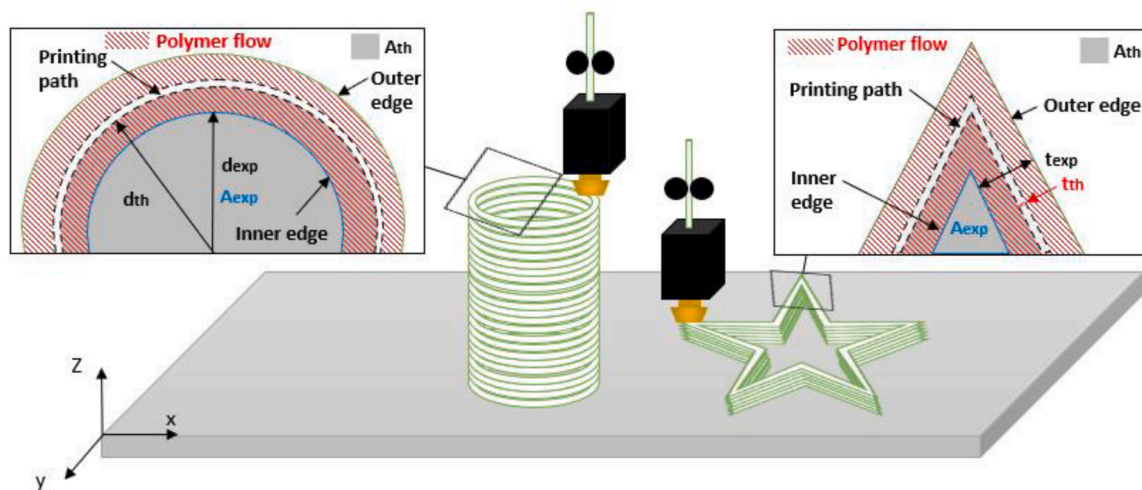**Fig. 1.** Parameters considered to quantify set and measured printed area for both circular and polygonal sections. The red hatched area represents polymer flow along printing while the dark area defines the theoretical area depending on the printed pattern. The dotted and blue line respectively delimit the printing path followed by the nozzle and the experimental area depending on the printed pattern.
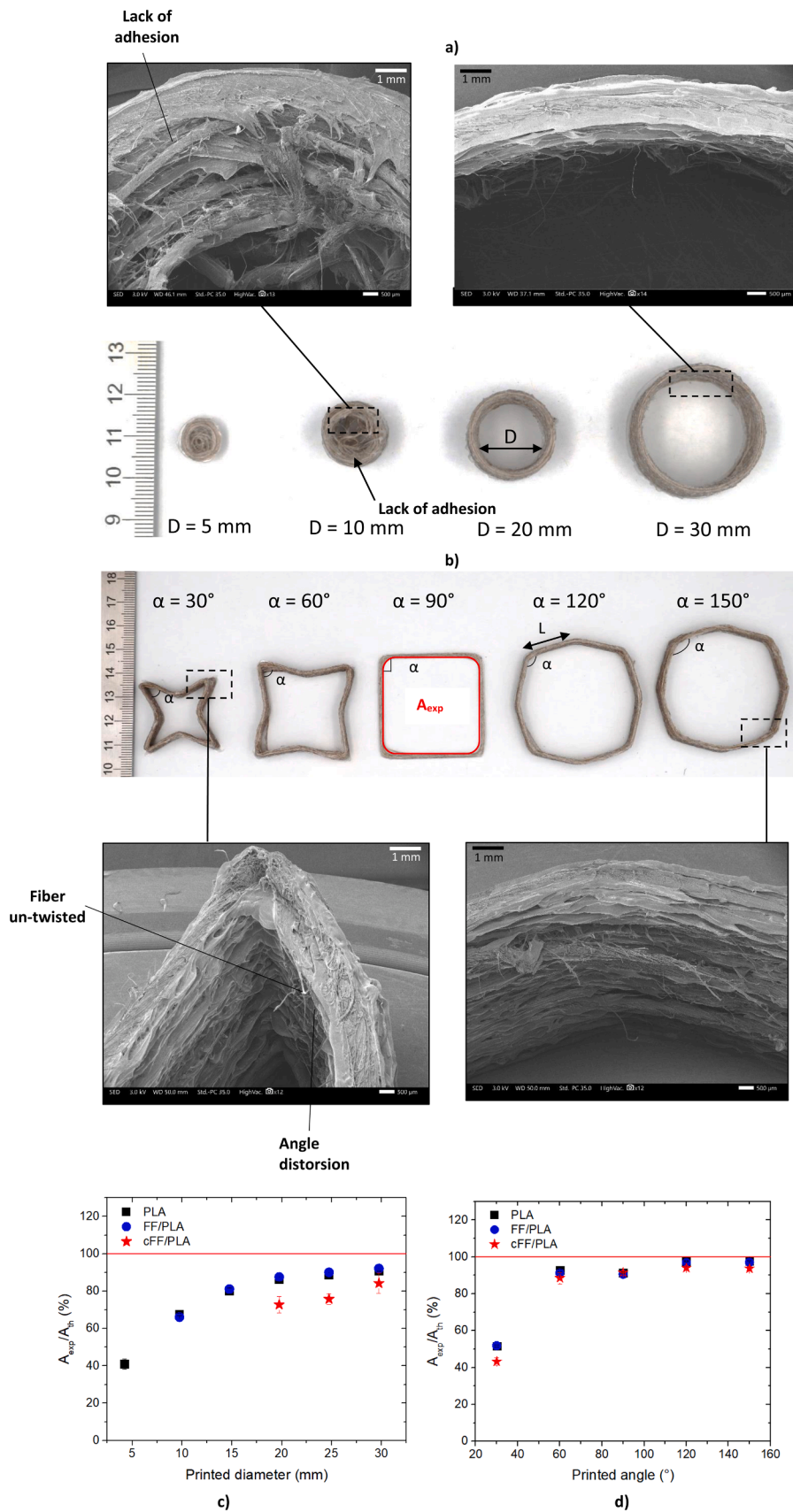
Fig. 2. cFF/PLA biocomposites with a) of circular shape b) of star/octagonal shape. Comparison between theoretical and experimental area as a function of the set c) diameter and d) angle.

concern. With a diameter between 20 and 30 mm, the printing fidelity for cFF/PLA is at its maximum, between 70 and 80% of the targeted programmed area. However, these values are lower than those obtained with pure PLA and FF/PLA biocomposites, for which fidelity of over 90% has been calculated. Furthermore, whatever the printed filament, none of the final structures reach 100% fidelity because of polymer flow occurring along the process (Fig. 1). Reducing the print diameter of the cellular pattern generates some issues (low bed adhesion, distortion angle) for cFF/PLA, to ensure proper filament deposition. The design of a cellular material (e.g. for the sandwich core) with cFF/PLA biocomposite may be limited to an internal diameter of 15 mm whereas the geometric limitations (i.e. minimum printable diameter) is lower for pure PLA and FF/PLA (about 5 mm with a similar fidelity range) for the set slicing and printing parameters. Similar tests were done with cCF/PA which exhibited a minimum achievable diameter of 8 mm by optimizing the filament size [15].

When the programmed diameter is less than 15 mm, the area could not be experimentally quantified correctly. The images indicate that the position of the deposited filament has significantly deviated from the initial circular position, instructed by the print path, towards the central area of the shape. This deviation is a likely result of short time dedicated to matrix solidification on previous layer, that is further exacerbated by an increase in tangential stresses with respect to the bonded area. This tangential stress results from the direction of movement of the nozzle in relation to the print path. Another reason for this deviation on the material deposition may be the result of a mismatch between the filament diameter (d = 0.4 – 0.6 mm) and the nozzle diameter (0.9 mm). The dimensional discrepancy between the nozzle and the filament has been technically needed in order to reduce filament damage during printing. A smaller nozzle has been tested before but it tends to results in either clogs or breakage of the filament due to the increased shear stress.

A similar strategy for nozzle sizing is already used in a commercial printer with continuous carbon fiber composites [18] where the nozzle diameter is 1 mm with a filament diameter of about 0.35 mm. This difference increases the degree of freedom of the filament during deposition, which affects the level of geometric precision that can be achieved over the printed cylinder shape.

In considering the influence of the programmed angle, it is essential to note that the length between the angles (L) was kept constant for this test to ensure a similar "length of adhesion" before applying the change in nozzle direction. Fig. 2d shows that the relatively high printing fidelity (around 90%) of cFF/PLA is observed at around 60°, which is very similar to pure PLA and FF/PLA biocomposites. It is also important to notice that there is a large difference in material stiffness ($E11_{PLA}$ = 3.1 ± 0.3 GPa, $E11_{cFF/PLA}$ = 15.8 ± 2.1 GPa) [1,16] but a similar range of printed filaments and quadratic moments that influence geometric bending stiffness.

Below α = 60°, a large discrepancy between the target tool-path geometry and the measurements of the printed sample is observed. This deviation occurs due to the lack of adhesion with the printing bed or between the vertical layers. Lower angles induce more radical changes in the direction and position in which the filament is deposited, which can generate greater in-plane tangential stress. Indeed, depending on their relative position within the bundle, the elementary flax fibers can be subjected to damage by buckling due to compressive stress. Flax fiber and all natural fibers are known to be prone to buckling failure due to their internal microstructure [19]. Similar observations have been made on cCF/PA parts [18,20].

4. Conclusion

In line with the ongoing development of 3D-printed biocomposites reinforced with continuous natural fibers, a first insight into the design limitation of tight angle and small size geometric features with small circular diameters has been proposed. These are geometric considerations that can have great impact in the design of periodic cellular

patterns and lattices for functional applications. It is interesting to note that shapes with non-acute angles can be achieved in a similar way between cFF/PLA, pure PLA and FF/PLA and should therefore be preferred to circular pattern design.

The observed variations between the programmed and experimental observations are assumed to be mainly due to:

- Relatively high in-plane stiffness of cFF/PLA due to biocomposite composition (fiber type and content).
- Twisted structure of flax yarns that may imply damage and reduce the strain accommodation of single fibers within the filament flexibility during printing.
- The uneven stress loading of the elementary fibers within the yarn that promotes the buckling of the fibers at acute angle.
- Limitations of interlayer bonding that result from the above-mentioned fibers characteristics but also due to the dimensional tolerances needed in the nozzle selection where the nozzle size is much larger than the fibers.

It is important to keep in mind that these results were obtained for specific printing and slicing parameters of which an adjustment might modify the printing quality. Further developments should be done to promote greater fidelity of cFF/PLA biocomposites but limiting the reduction in intrinsic material stiffness that is required for semi-structural application. Thus, the production of smaller diameter (<0.5 mm) cFF/PLA filaments may be relevant, especially if rovings are used instead of twisted yarns. Roving will help the single fiber to conform during printing. In combination, the nozzle diameter should be as close as possible to the filament diameter. The temperature-printing speed coupling could also be adjusted as it governs viscoelastic properties of the matrix and adhesion process in order to optimize matrix deposition and reduce structural flaws. Finally, geometric limitations can also be overcome by incorporating an offset factor during programing/design that can account for such deviations. This offset could be similar to factors used to accommodate for polymer shrinkage that results in warpage issues for certain materials. Thus, taking the fidelity ratio into account during programing can expand the design space for cFF/PLA 3D printed biocomposites with cellular patterns.

Declaration of Competing Interest

The authors declare no conflict of interests.

Data Availability

Data will be made available on request.

References

[1] A. Le Duigou, D. Correa, M. Ueda, R. Matsuzaki, M. Castro, « A review of 3D and 4D printing of natural fibre biocomposites », Mater. Des. 194 (2020), 108911 https://doi.org/10.1016/j.matdes.2020.108911.
[2] A. Le Duigou, A. Barbé, E. Guillou, M. Castro, « 3D printing of continuous flax fibre reinforced biocomposites for structural applications », Mater. Des. 180 (2019), 107884 https://doi.org/10.1016/j.matdes.2019.107884 oct.
[3] A. L. Duigou, R. Matsuzaki, M. Ueda, et M. Castro, « 4D printing of continuous flax-fibre based hygromorph biocomposites », p. 32.
[4] S. Ahn, M. Montero, D. Odell, S. Roundy, P.K. Wright, « Anisotropic material properties of fused deposition modeling ABS », Rapid Prototyp. J. 8 (4) (oct. 2002) 248–257. https://doi.org/10.1108/13552540210441166.

[5] S. Wolff, T. Lee, E. Faierson, K. Ehmann, J. Cao, « Anisotropic properties of directed energy deposition (DED)-processed Ti–6Al–4V », J. Manuf. Process. 24 (2016) 397–405. https://doi.org/10.1016/j.jmapro.2016.06.020, oct.

[6] A.K. Sood, R.K. Ohdar, S.S. Mahapatra, « Parametric appraisal of mechanical property of fused deposition modelling processed parts », Mater. Des. 31 (1) (2010) 287–295. https://doi.org/10.1016/j.matdes.2009.06.016, janv.

[7] S. Poppinga, et al., « Toward a new generation of smart biomimetic actuators for architecture », Adv. Mater. 30 (19) (2018), 1703653 https://doi.org/10.1002/adma.201703653.

[8] S. Poppinga, D. Correa, B. Bruchmann, A. Menges, T. Speck, « Plant movements as concept generators for the development of biomimetic compliant mechanisms », Integr. Comp. Biol. 60 (4) (2020) 886–895. https://doi.org/10.1093/icb/icaa028, oct.

[9] D. Correa, et al., « 4D pine scale: biomimetic 4D printed autonomous scale and flap structures capable of multi-phase movement », Philos. Trans. R. Soc. Math. Phys. Eng. Sci. 378 (2167) (2020), 20190445 https://doi.org/10.1098/rsta.2019.0445.

[10] A. Mader, M. Langer, J. Knippers, O. Speck, « Learning from plant movements triggered by bulliform cells: the biomimetic cellular actuator », J. R. Soc. Interface 17 (169) (2020), 20200358 https://doi.org/10.1098/rsif.2020.0358 août.

[11] B.I. Oladapo, S.O. Ismail, A.V. Adebiyi, F.T. Omigbodun, M.A. Olawumi, D. B. Olawade, « Nanostructural interface and strength of polymer composite scaffolds applied to intervertebral bone », Colloids Surf. Physicochem. Eng. Asp. 627 (2021), 127190 https://doi.org/10.1016/j.colsurfa.2021.127190 oct.

[12] U. Morales, A. Esnaola, M. Iragi, L. Aretxabaleta, J. Aurrekoetxea, « The effect of cross-section geometry on crushing behaviour of 3D printed continuous carbon fibre reinforced polyamide profiles », Compos. Struct. 274 (2021), 114337 https://doi.org/10.1016/j.compstruct.2021.114337 oct.

[13] M. Yamawaki, Y. Kouno, « Fabrication and mechanical characterization of continuous carbon fiber-reinforced thermoplastic using a preform by three-dimensional printing and via hot-press molding », Adv. Compos. Mater. 27 (2) (2018) 209–219. https://doi.org/10.1080/09243046.2017.1368840.

[14] K. Sugiyama, R. Matsuzaki, M. Ueda, A. Todoroki, Y. Hirano, « 3D printing of composite sandwich structures using continuous carbon fiber and fiber tension », Compos. Part Appl. Sci. Manuf. 113 (2018) 114–121. https://doi.org/10.1016/j.compositesa.2018.07.029.

[15] R. Matsuzaki, et al., « Effects of set curvature and fiber bundle size on the printed radius of curvature by a continuous carbon fiber composite 3D printer », Addit. Manuf. 24 (2018) 93–102. https://doi.org/10.1016/j.addma.2018.09.019, déc.

[16] T. Fruleux, M. Castro, P. Sauleau, R. Matsuzaki, A. Le Duigou, « Matrix stiffness: a key parameter to control hydro-elasticity and morphing of 3D printed biocomposite », Compos. Part Appl. Sci. Manuf. (2022), 106882 https://doi.org/10.1016/j.compositesa.2022.106882.

[17] A. Le Duigou, G. Chabaud, R. Matsuzaki, M. Castro, « Tailoring the mechanical properties of 3D-printed continuous flax/PLA biocomposites by controlling the slicing parameters », Compos. Part B Eng. 203 (2020), 108474 https://doi.org/10.1016/j.compositesb.2020.108474 déc.

[18] G. Chabaud, M. Castro, C. Denoual, A. Le Duigou, « Hygromechanical properties of 3D printed continuous carbon and glass fibre reinforced polyamide composite for outdoor structural applications », Addit. Manuf. 26 (2019) 94–105. https://doi.org/10.1016/j.addma.2019.01.005, mars.

[19] H. L. Bos, « Tensile and compressive properties of flax fibres for natural fibre reinforced composites », p. 10.

[20] H. Shiratori, A. Todoroki, M. Ueda, R. Matsuzaki, Y. Hirano, « Mechanism of folding a fiber bundle in the curved section of 3D printed carbon fiber reinforced plastics », Adv. Compos. Mater. 29 (3) (2020) 247–257. https://doi.org/10.1080/09243046.2019.1682794.\.